

Supporting Information

Efficient all polymer active layers with long-range ordered 1D p-n nanoheterojunctions confirmed by TEM tomography

Seon-Mi Jin,^a Jun Ho Hwang,^a Jaehyeong Park,^a Du Hyeon Ryu,^b BongSoo Kim,^c Chang Eun Song^b and Eunji Lee^{*,a}

^a School of Materials Science and Engineering, Gwangju Institute of Science and Technology (GIST), Gwangju 61005, Republic of Korea

^b Energy Materials Research Center, Korea Research Institute of Chemical Technology (KRICT), Daejeon 34114, Republic of Korea

^c Department of Chemistry, Ulsan National Institute of Science and Technology (UNIST), Ulsan 44919, Republic of Korea

Corresponding Authors

E-mail: eunjilee@gist.ac.kr

1. Materials and Instruments All commercially available reagents were used without further purification unless otherwise indicated. PTB7-Th was purchased from 1-material. 1.6 M *n*-butyllithium (BuLi) solution in hexanes, 1.0 M trimethylstannyl chloride (TMSnCl) solution in tetrahydrofuran (THF), tetrakis(triphenylphosphine)palladium(0) (Pd(PPh₃)₄), anhydrous toluene, anhydrous *N,N*-dimethylformamide (DMF), anhydrous THF, zinc acetate dehydrate, ethanolamine, 2-methoxyethanol, ethoxylated polyethyleneimine (PEIE), and MoO₃ were purchased from Sigma-Aldrich Chemical Co. Ltd. 4,9-Dibromo-2,7-bis(2-hexyldecyl)benzo[*lmn*][3,8]phenanthroline-1,3,6,8(2H,7H)-tetraone (NDI-Br) was purchased from Sunatech Inc. Chloroform was purchased from Daejung. 2,2'-bithiophene was purchased from Alfa Aesar. Deuterated chloroform (CDCl₃) for measurement of ¹H NMR spectrum was purchased from Cambridge Isotope Laboratories. THF was dried over sodium and benzophenone prior to use. Toluene and DMF, used as solvents for polymerization, were separately degassed by Freeze-Pump-Thaw three cycling and added to the reaction mixture.

Nuclear Magnetic Resonance Spectroscopy (NMR). All ¹H NMR spectra were recorded at 300 MHz, using CDCl₃ as a solvent, unless otherwise stated. The chemical shifts of all ¹H NMR spectra are referenced to the residual signal of CDCl₃ (δ 7.26 ppm) by Bruker 300 MHz NMR instrument. All coupling constants, *J*, are reported in Hertz (Hz).

Gel Permeation Chromatography (GPC). The molecular weights and PDI of polymers were determined by an Agilent GPC system (GPC 1200 system, Agilent Technologies, Santa Clara, USA). *o*-Dichlorobenzene was used as the eluent. The molecular weight (*M_w*) and the polydispersity index (PDI) were calculated using monodisperse polystyrene standards.

UV-Vis Spectrometer. Absorption spectra were obtained using a UV-Vis spectrometer (UH5300, HITACHI, Tokyo, Japan).

Polarized Optical Microscopy (POM). POM was performed on specimens prepared using a glass substrate without a MoO_x/Ag top electrode. The optical texture of the samples was observed using a Nikon LV100POL polarized optical microscope (Nikon, Japan) with a full-wave plate ($\lambda = 530$ nm) inserted at a 45° angle to the polarizers. Images were recorded using a Nikon DS-R1i CCD camera.

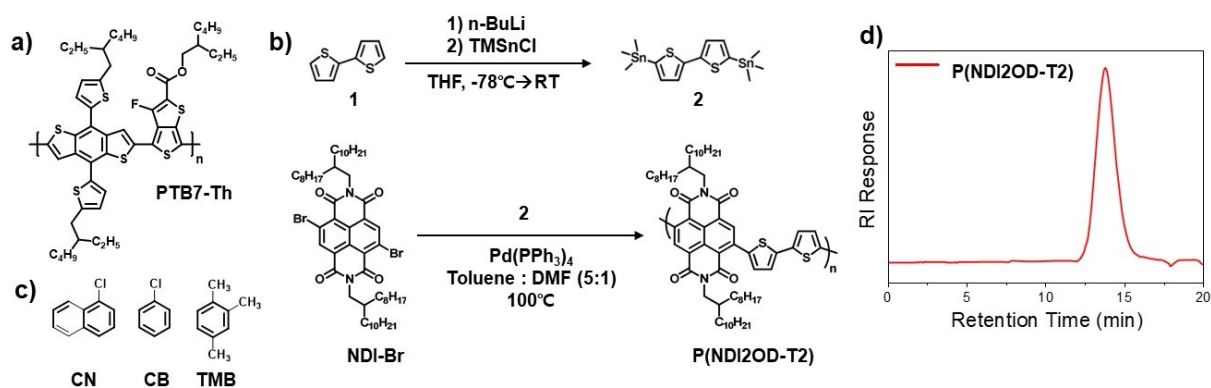
Transmission Electron Microscopy (TEM). For TEM samples, the donor and acceptor polymers blend solutions were spin-coated on a glass substrate, covered with water-soluble PEDOT:PSS. PEDOT:PSS was spun at 5000 rpm for 20 sec from a solution. All thin-films on PEDOT:PSS are floated off in deionized (DI) water and transferred on a carbon-coated copper grid. The images were obtained on a JEM-1400 (JEOL, Japan) operating at 120 kV, and the images were acquired with Veleta (with a megapixel) and Tengra (with 5.3 megapixels) CCD cameras (EMSIS, Germany).

Current density-Voltage (*J-V*) Measurement System. The *J-V* characteristics were recorded using a computer-controlled Keithley 236 Source-Measure unit (Keithley Instruments, Inc., USA). The PSC performances were measured under the illumination of AM 1.5 G, 100 mW/cm², using a solar simulator (Newport-Oriel Instruments, USA) with a Xenon light source.

2. Synthesis

Synthesis of 5,5'-bis(trimethylstannyl)-2,2'-bithiophene [2].^{S1,2} **1** (2,2'-bithiophene, 1.06 g, 6.40 mmol) was dissolved in distilled THF (60 mL). The solution was cooled down to -78 °C and 1.6 M *n*-BuLi solution in hexanes (9.6 mL, 15.36 mmol) was added dropwise. The reaction mixture was warmed up slowly and stirred at RT for 1 h, and then cooled down to -78 °C. 1 M TMSnCl solution in THF (15.3 mL, 15.36 mmol) was added dropwise to the reaction solution, which was then warmed up to RT and stirred for 18 h. The reaction mixture was poured into water and the organic layer was washed with water (50 mL) three times. The organic layer was dried over MgSO₄ and the filtered solution was concentrated by rotary evaporation. After the crude product was diluted with DCM (0.5 mL), methanol (10 mL) was poured into the solution. The mixture was stored in a -25 °C refrigerator overnight. The white solid precipitate was formed, which was then filtered to yield a pure product (2.27 g, 71% yield). ¹H NMR (300 MHz, CDCl₃): δ = 7.27 (d, *J* = 3.3 Hz, 2H), 7.08 (d, *J* = 3.3 Hz, 2H), 0.38 (s, 18H).

Synthesis of poly([N,N'-bis(2-decyltetradecyl)naphthalene-1,4,5,8-is-(dicarboximide)-2,6-diyl]-alt-5,5'-(2,2'-bithiophene)), P(NDI2OD-T2).^{S1,2} NDI-Br (0.50 g, 0.51 mmol), 5,5'-bis(trimethylstannyl)-2,2'-bithiophene (0.25 g, 0.51 mmol), and Pd(PPh₃)₄ (0.02 g, 0.02 mmol) were added to a flame-dried 25 mL round-bottom flask. Degassed toluene (8.6 mL) and degassed DMF (1.7 mL) were added to the reaction flask. The reaction solution was heated up to 100 °C slowly and stirred at 100 °C for 2 h under an N₂ atmosphere. Next, the reaction solution was cooled to RT and diluted with chloroform (10 S-8 mL), and filtered through Celite. Then the crude polymer solution was precipitated into ethanol (200 mL). The precipitated polymers were filtered through a thimble tube and then purified by Soxhlet extraction with methanol, acetone, hexane, cyclohexane, dichloromethane, and chloroform. The chloroform fraction was precipitated in methanol. The resulting polymer was filtered and dried under vacuum to yield polymer P(NDI2OD-T2) (222.8 mg, 44% yield). ¹H NMR (300 MHz, CDCl₃): δ = 8.92-8.15 (4H), 1.48-0.79 (82H). GPC (*M*_n = 83,000 Da, *M*_w = 170,000 Da, PDI = 2.05).



Scheme S1. Molecular structures of (a) PTB7-Th polymer, (b) P(NDI2OD-T2), and (c) processing solvents. (d) GPC traces of P(NDI2OD-T2) with *o*-dichlorobenzene as eluent at 150 °C.

Table S1 Characteristics of synthesized n-type P(NDI2OD-T2) polymer used in this study

Polymer	<i>M</i> _n (g/mol)	<i>M</i> _w (g/mol)	PDI
P(NDI2OD-T2)	83,000	170,000	2.05

3. Methods

Solvent Selection for polymer crystallization-driven assembly. The crystallization-driven assembly of P(NDI2OD-T2) is highly sensitive to the compatibility between P(NDI2OD-T2) and used solvents; the mutual P(NDI2OD-T2)–solvent interactions were predicted by considering the Hansen solubility parameters (HSPs). The HSPs of P(NDI2OD-T2) and the solvents used in this study can be calculated according to the group contribution theory.^{S1} The HSP space (R_a) was evaluated using eq. 1.^{S2}

$$R_a^2 = 4(\delta_{d1} - \delta_{d2})^2 + (\delta_{p1} - \delta_{p2})^2 + (\delta_{h1} - \delta_{h2})^2 \quad \text{----- (1)}$$

Here, δ_d , δ_p , and δ_h represent solubility parameters of the dispersion force, dipolar intermolecular force, and hydrogen bonding, respectively. Each of the solubility parameters (δ_d , δ_p , and δ_h) for P(NDI2OD-T2) and the solvents, and the corresponding R_a value, are represented in Table S2. A lower R_a indicates good miscibility between P(NDI2OD-T2) and the used solvents.

Table S2 Physicochemical properties and solubility parameters of P(NDI2OD-T2) and various solvents. Hansen solubility parameters (HSPs) for P(NDI2OD-T2), chloronaphthalene (CN), 1,2,4-trimethylbenzene (TMB), and *o*-dichlorobenzene (CB)

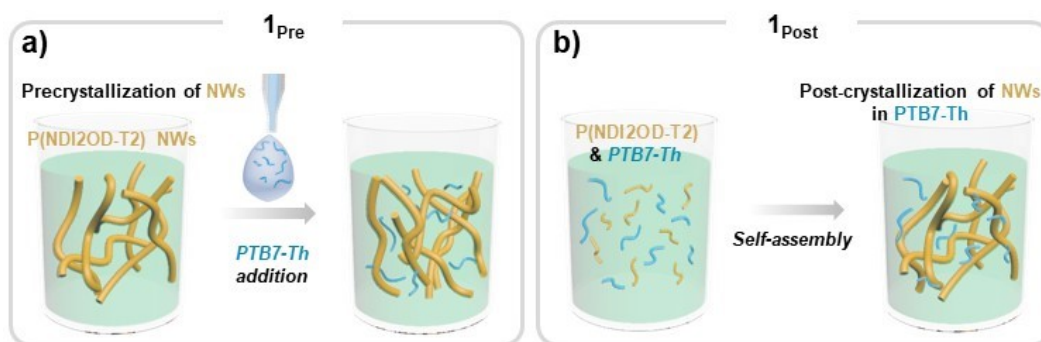
Solvents	P(NDI2OD-T2)	CN	TMB	CB
Density (g cm ⁻³)	-	1.19	0.88	1.11
Boiling point (°C)	-	259	169	132
δ (MPa ^{1/2})	19.1	21.2	18.1	19.6
δ_d^a (MPa ^{1/2})	17.7	20.5	18	19
δ_p^b (MPa ^{1/2})	5.9	4.9	1	4.3
δ_h^c (MPa ^{1/2})	4.3	2.5	1	2
R_a^d (P(NDI2OD-T2))	-	6.9	11.8	6.2
Polarizability	-	19.3	15.1	12.4

1_{Pre} (Precrystalline P(NDI2OD-T2) NWs mixed with PTB7-Th). 10 mg of P(NDI2OD-T2) was dissolved in 1 mL TMB under agitation. During the dissolution process, the solution was protected from light and ambient air to avoid chemical oxidation and/or the photo-oxidation of the polymer. And then, 10 mg of PTB7-Th was added into P(NDI2OD-T2) NWs solution in TMB.

1_{Pre-H} (Pre-crystalline P(NDI2OD-T2) NWs by heating and cooling mixed with PTB7-Th). 10 mg of P(NDI2OD-T2) was dissolved in 1 mL TMB under agitation. During the dissolution process, the solution was protected from light and ambient air to avoid the chemical oxidation and/or the photo-oxidation of the polymer. In order to completely dissolve the P(NDI2OD-T2) polymer, the solution strung at 100 °C was slowly cooled to room temperature. Then, 10 mg of PTB7-Th was added to the P(NDI2OD-T2) NWs solution of TMB.

1-T (Thermal annealing of cast film 1_{Pre-H}). Solution 1_{Pre-H} was spin-coated at 1500 rpm for 15 sec to obtain the pristine films. The prepared film was annealed at 150 °C for 30 min.

1_{Post} (Crystallization of P(NDI2OD-T2) NWs in PTB7-Th). 10 mg of PTB7-Th and 10 mg of P(NDI2OD-T2) were dissolved in 1 mL TMB under agitation. During the dissolution process, the solution was protected from light and ambient air to avoid chemical oxidation and/or the photo-oxidation of the polymers. After 1 d, the crystallization of the P(NDI2OD-T2) polymer in PTB7-Th TMB solution was completed.



Scheme S2 Schematic representation of two different processes for the preparation of PTB7-Th/P(NDI2OD-T2) NWs TMB solution; (a) precrystalline and (b) postcrystalline NWs solutions are referred to as 1_{Pre} and 1_{Post} , respectively.

2 (Blends of PTB7-Th and P(NDI2OD-T2)). 10 mg of PTB7-Th and 10 mg of P(NDI2OD-T2) were dissolved in 1 mL CB under agitation. During the dissolution process, the solution was protected from light and ambient air to avoid chemical oxidation and/or the photo-oxidation of the polymers.

Fabrication of PTB7-Th:P(NDI2OD-T2) Thin-Films. The glass substrates were sequentially cleaned with DI water, acetone, and isopropanol, and dried in an oven at 120 °C overnight. Then, the substrates were treated with UV/ozone for 15 min. A thin film of PEDOT:PSS was spin-coated at 5000 rpm for 20 sec and annealed at 150 °C for 15 min. The all-polymer blend solutions (PTB7-Th:P(NDI2OD-T2) = 1:1 (w/w), 20 mg/mL of CB and TMB) were spin-coated at 1200 rpm for 15 sec on the PEDOT:PSS. The thickness of the photoactive films was fixed at about ~100 nm.

Device Fabrication and Characterization. Inverted BHJ APSCs devices were fabricated with ITO/ZnO/PEIE/PTB7-Th:P(NDI2OD-T2) or PTB7-Th:P(NDI2OD-T2) NW/MoO_x/Ag structures. The ITO glass substrates were sequentially cleaned with deionized water, acetone, and isopropanol. UV/ozone treatment was performed on the ITO substrates for 20 min. Zinc oxide (ZnO) nanoparticles in isopropanol were spin-coated onto the ITO glass substrates at 5000 rpm for 20 sec and dried at 120 °C for 10 min. PEIE solution was spin-coated at 5000 rpm for 20 sec and dried at 120 °C for 10 min. Conventional and NW-based blend solutions (PTB7-Th:P(NDI2OD-T2)=1:1 w/w, 20 mg/mL of CB and TMB, respectively) were spin-coated in the glove box at 1000 rpm for 10 sec on the PEIE/ZnO-coated ITO glass. The device fabrication was completed by thermal evaporation of 10 nm MoO_x and 100 nm Ag as the anode under vacuum at a base pressure of 3×10^{-6} Torr. APSCs efficiencies were characterized under simulated 100 mW/cm² with AM 1.5G irradiation from a Xenon arc lamp. Simulator irradiance was characterized using a calibrated spectrometer, and the illumination intensity was set using an NREL-certified silicon diode with an integrated KG1 optical filter. The air stability of the devices was tested as a function of the exposure time under a sunlight environment of 100 mW/cm² with AM 1.5G in air.

Solar Cell Properties Measurements. The photovoltaic performance of the devices was characterized by a 150 W Xenon lamp-based solar simulator (McScience Inc., Republic of Korea) using a Keithley 2400 source meter under AM 1.5G irradiation (100 mW/cm²). The EQE curves were obtained by a spectral measurement system (K3100 IQX, McScience Inc.). The light source (a 300 W xenon arc lamp) was used with a monochromator (Newport) and an optical chopper (MC 2000 Thorlabs).

Carrier Mobility Measurement.^{S5} The hole and electron mobilities of films were measured with ITO/PEDOT:PSS/photoactive film/Au and ITO/ZnO/PEIE/photoactive film/Ca/Al for the hole-only and electron-only devices, respectively. The measurement involved obtaining current density-voltage (J - V) characteristics and fitting the results to a space-charge limited current (SCLC) form. The hole mobilities were calculated using the SCLC model, which is described by: $J = 9\epsilon_0\epsilon_r\mu_h V^2/8L^3$, where J is the current density, L is the film thickness, μ_h is the hole mobility, ϵ_r is the relative dielectric constant of the transport medium, ϵ_0 is the permittivity of free space (8.85×10^{-12} F m⁻¹), V is the internal voltage in the device, and $V = V_{\text{appl}} - V_{\text{bi}} - V_r$. Here, V_{appl} represents the applied voltage to the device, V_{bi} is the built-in voltage due to the relative work function difference between the electrodes, and V_r is the voltage drop caused by contact resistance and series resistance between the electrodes.

Operation of GTFiber Software.^{S6} The use of GTFiber software includes four steps, corresponding to the four areas marked on the operation interface of the software. Enter the image's width in nanometers and wait for the original image to appear. Note that the software identifies fiber-like objects as white. Choosing the right filter parameters is important for obtaining credible processing results. This step includes six stages. The theory of each stage and the effect of each parameter has been well-documented by Persson et al.^{S6} Typically, the orientation smoothing should be set to the width of a single fiber-like object. The top hat size should be greater than or equal to the smallest width of fiber-like objects. The values of other parameters can be tried over and over to determine what work best for the application. The values used in this work have been shown in Fig. 3 and Fig. S8. To view the result after any filtering stage, check the "Display Result" box. Click "Run Filter" and wait for the progress bars to complete and disappear. The results of each image filtering stage will appear if the corresponding "Display Result" boxes have been checked. Click "Orientation Map" to display figures for the calculated results. An orientation map with the alignment directions of fiber-like objects marked with false color, and an orientation distribution map will appear at the same time.

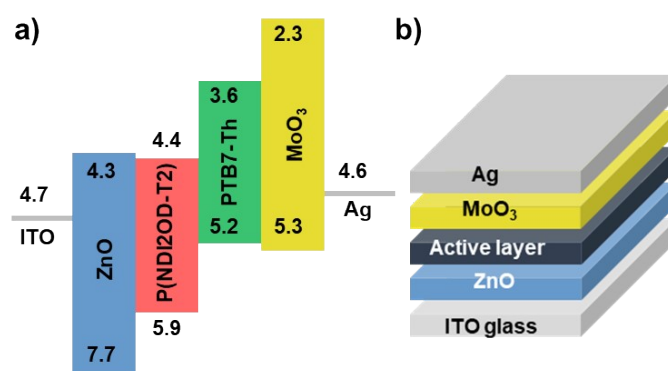


Fig. S1 (a) Energy level diagram of the materials used in this study. (b) The device structures of all-polymer solar cells (APSCs).

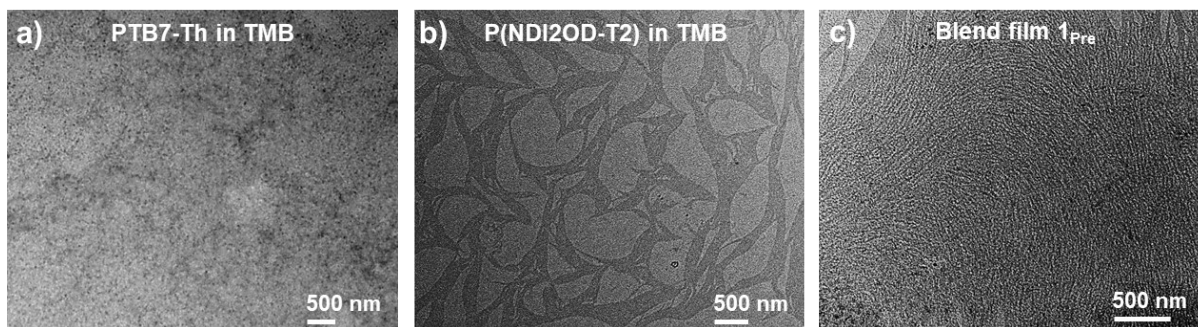


Fig. S2 TEM images of (a) neat PTB7-Th and (b) neat P(NDI2OD-T2) films drop casting from a 0.1 mg/ml solution in TMB. (c) TEM image of photoactive film as-cast from $\mathbf{1}_{\text{Pre}}$ TMB.

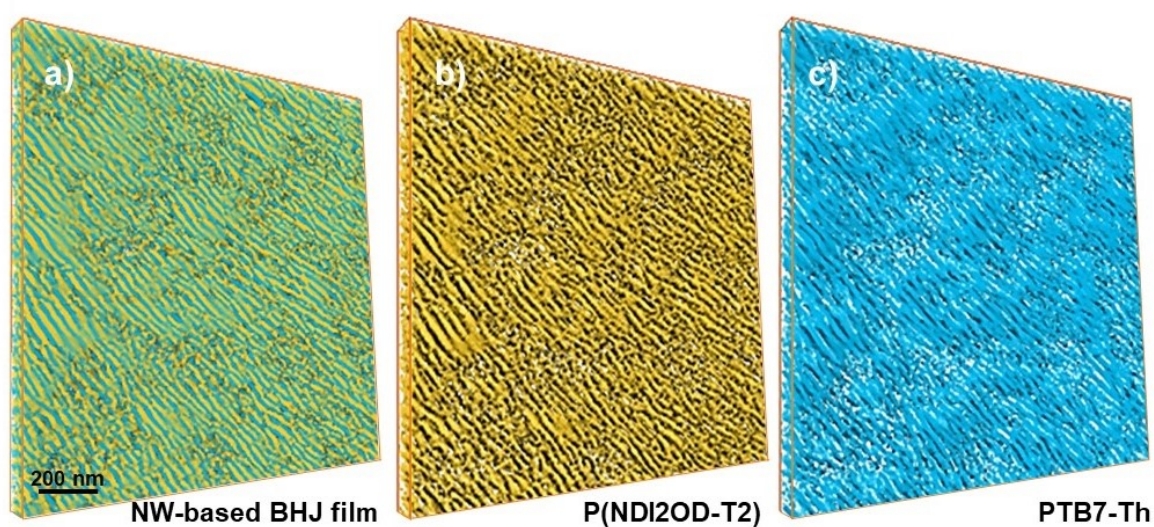


Fig. S3 (a) Tomograms of large area photoactive film cast from $\mathbf{1}_{\text{Pre}}$ solution. Domains of (b) P(NDI2OD-T2) and PTB7-Th extracted from a), labelled in yellow and sky blue, respectively.

Table S3 Detailed experimental conditions for tomography

Film	Thin-film cast from $\mathbf{1}_{\text{Pre}}$
Angular sampling	$-68^\circ \sim +70^\circ$
Increments angle	2°
Magnification	$30,000 \times$
Pixel size	2.3 nm for images

Table S4 The d -spacing and coherence length (L_c) obtained from out-of-plane and in-plane line cut profiles of thin films as-cast from solutions.

Films	d -spacing ₍₁₀₀₎ (Å) ^a	d -spacing ₍₀₁₀₎ (Å) ^b	$L_{c(100)}$ (Å) ^a	$L_{c(010)}$ (Å) ^b
1_{Pre}	26.3	3.95	161.3	25.4
1_{Pre-H}	25.4	3.95	172.7	27.1
1-T	25.4	3.87	198.1	28.3
1_{Post}	25.5	3.98	147.7	19.4
2	26.1	3.83	155.1	14.8

^aEstimated by the (100) peak position and full-width at half-maximum (FWHM). ^bEstimated by the (010) peak position and FWHM.

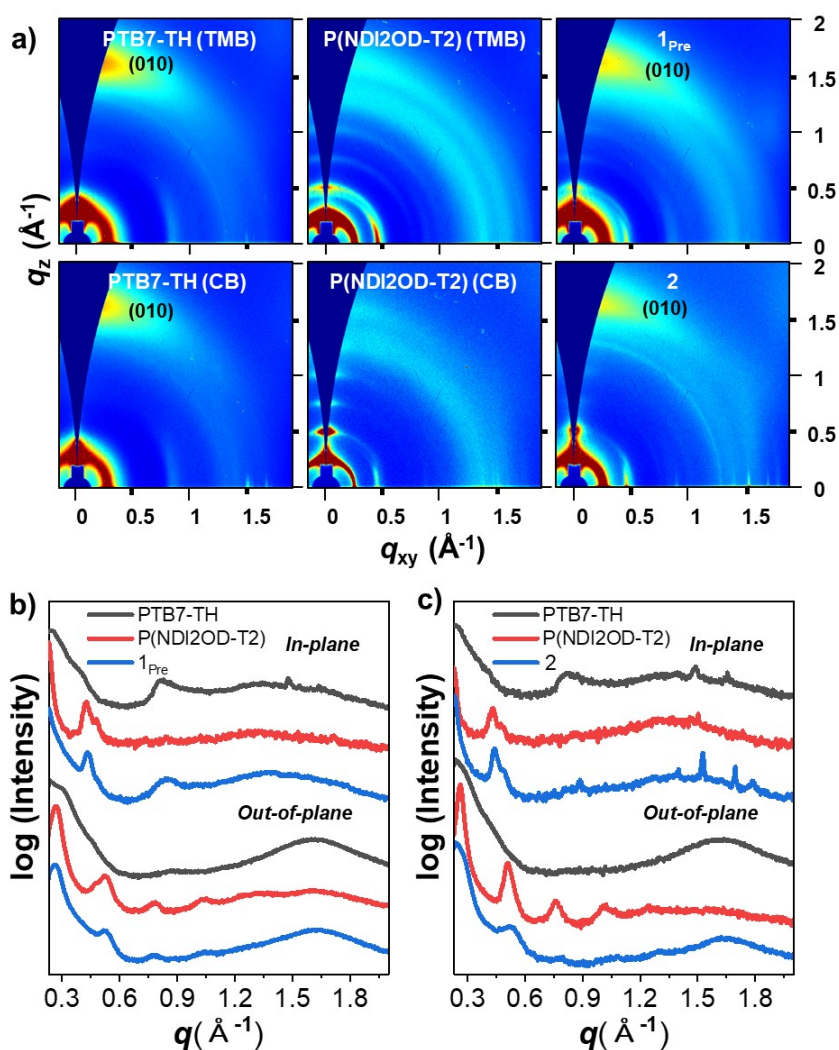


Fig. S4 (a) GIWAXS patterns of thin-films as-cast from PTB7-Th, P(NDI2OD-T2), and PTB7-Th:P(NDI2OD-T2) blend solutions of **1_{Pre}** and **2** using CB and TMB solvents, respectively. (b,c) In-plane and out-of-plane line cut (q_{xy} and q_z) profiles from the 2D GIWAXS patterns of **1_{Pre}** and **2**.

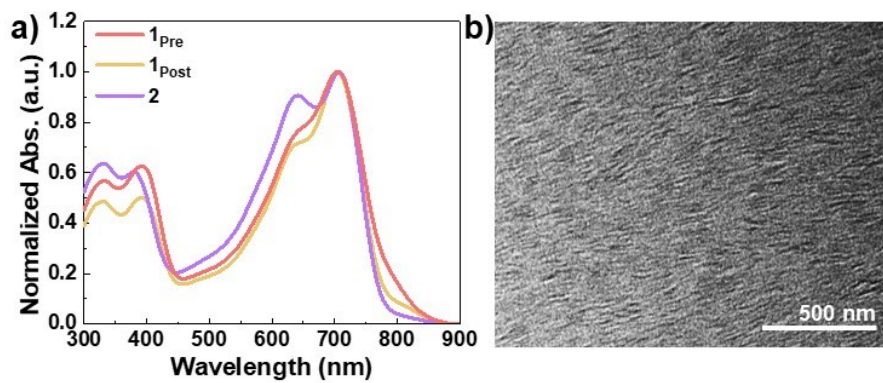


Fig. S5 (a) UV-Vis absorption of PTB7-Th/P(NDI2OD-T2) solutions using TMB (for $\mathbf{1}_{\text{Post}}$ and $\mathbf{1}_{\text{Post}}$) and CB (for $\mathbf{2}$) solvents. (b) TEM image of the thin film obtained through spin-casting from a $\mathbf{1}_{\text{Post}}$ TMB solution.

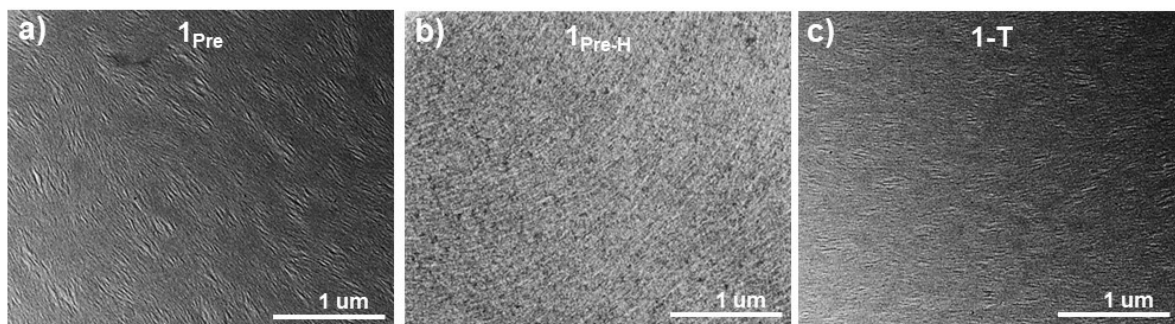


Fig. S6 TEM images of PTB7-Th/P(NDI2OD-T2) photoactive films obtained from (a) $\mathbf{1}_{\text{Pre}}$, (b) $\mathbf{1}_{\text{Pre-H}}$, and (c) $\mathbf{1-T}$, respectively.

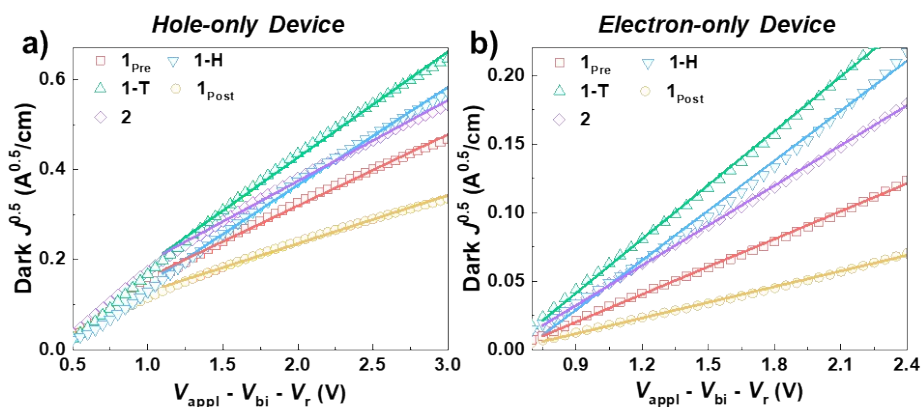


Fig. S7 Dark $J_{0.5}$ - V curves of the (a) hole-only and (b) electron-only SCLC devices with the structure of ITO/PEDOT:PSS/photoactive layer film/Au and ITO/ZnO NPs/PEIE/photoactive layer film/Ca/Al, respectively.

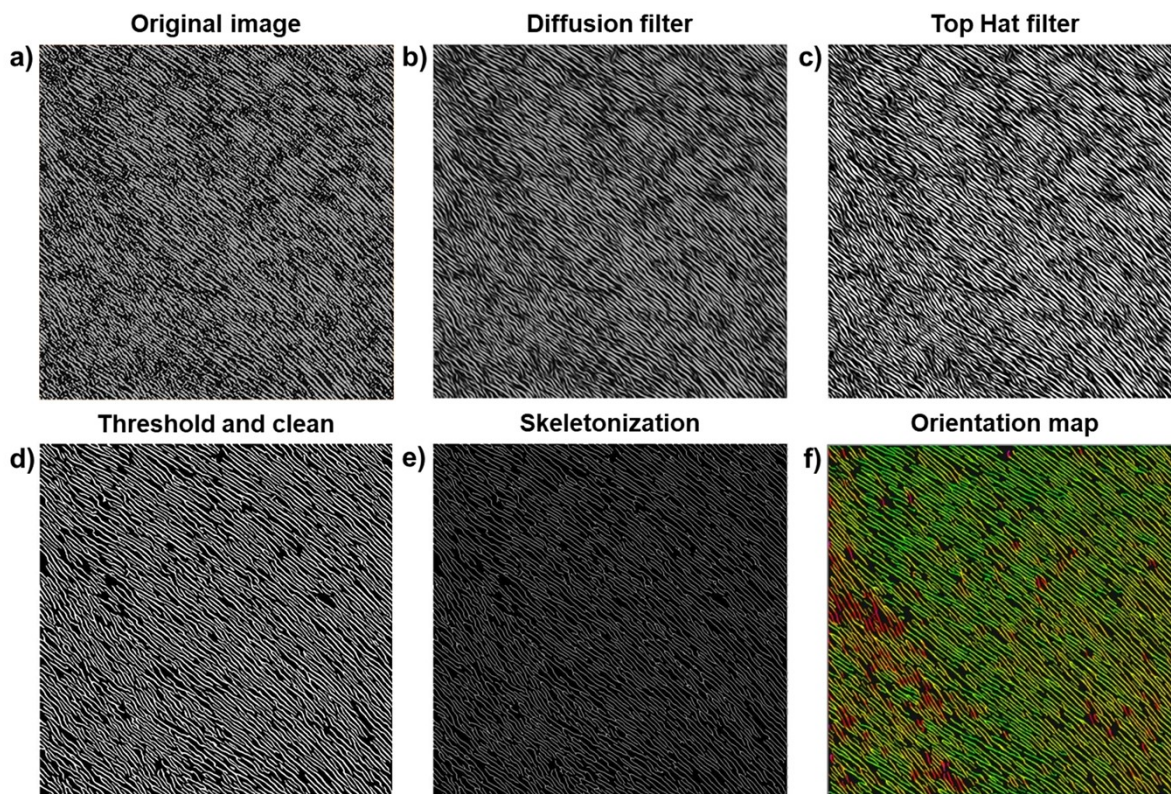


Fig. S8 Overview of image processing applied to obtain orientation maps using GTFiber software in the order of a) through f).

Material Reproduction Video S1. A video displaying the reconstructed 3D volume of a PTB7-Th/P(NDI2OD-T2) NWs-based thin film, showcasing the 1D arrangement of p-n nanoheterojunction in the large area.

References for Supporting Information

- S1. C.-H. Cho, H. Kang, T. E. Kang, H.-H. Cho, S. C. Yoon, M.-K. Jeon, B. J. Kim, *Chem. Commun.*, 2011, **47**, 3577.
- S2. M. J Kim, A.-R. Jung, M. Lee, D. Kim, S. Ro, S.-M. Jin, H. D. Nguyen, J. Yang, K.-K. Lee, E. Lee, M. S. Kang, H. Kim, J.-H. Choi, B. Kim, J. H. Cho, *ACS Appl. Mater. Interfaces*, 2017, **9**, 40503.
- S3. A. F. M. Barton, *CRC handbook of solubility parameters and other cohesion parameters*, CRC press, **1991**.
- S4. C. M. Hansen, *Hansen solubility parameters: a user's handbook*, CRC press, **2007**.
- S5. S. Oh, N. Khan, S.-M. Jin, H. Tran, N. Yoon, C. E. Song, H. K. Lee, W. S. Shin, J.-C. Lee, S.-J. Moon, E. Lee, S. K. Lee, *Nano Energy*, 2020, **72**, 104708.
- S6. N. E. Persson, M. A. McBride, M. A. Grover, E. Reichmanis, *Chem. Mater.*, 2017, **29**, 3.